Ligand Coordinate Analysis of SC-558 from the Active Site to the Surface of COX-2: A Molecular Dynamics Study

K. V. V. M. Sai Ram,[†] G. Rambabu,[‡] J. A. R. P. Sarma,*[,‡] and G. R. Desiraju*[,†]

School of Chemistry, University of Hyderabad, Hyderabad 500 046, India, and Informatics Division, GVK Biosciences Pvt. Ltd., 6-3-1192 Begumpet Hyderabad 500 016, India

Received April 22, 2005

We have performed a ligand coordinate analysis to monitor the movement of the inhibitor SC-558 from the active site of the COX-2 protein to the exterior using molecular dynamics techniques. This study provides an insight into the intermolecular interactions formed by the ligand during this journey. The published crystal structure of COX-2 with SC-558 in the active site (1cx2) was taken, and the ligand was moved incrementally in 13 steps. At each of these points on the path, exhaustive minimization and dynamics calculations were performed. The role of water was found to be important in these computations. An average structure was obtained from 250 conformations at each point and minimized. At each point on the path, the 10 lowest-energy conformations were also selected; a consideration of the average and lowest conformations provides fine details on the consistency of specific and strong interactions, and also on the geometry of the ligand. The movement of the ligand through the protein may be divided into three stages that are distinguished from each other because of energy and geometry discontinuities in both the ligand and the protein. The first of these covers the region between the active site and the point at 5.8 Å from it. The second, which covers the distance between 8.2 and 10.0 Å and is associated with maximum energetic and structural instability, is of critical importance. The third stage covers the distance between 10.5 Å and the exterior and represents a stage of increasing hydration and expulsion of the ligand from the protein. Our results provide a confirmation for the existence of a shallow cavity near the protein surface in which the ligand is bound reversibly. By examining the residues that show maximum mobility, one obtains an idea of the gating mechanism that governs the entry and exit of the protein into or from the deep pocket that contains the active site. We note, however, that the variation of the root-mean-square deviation of all residues begins to increase almost as soon as the ligand leaves the active site, and even before there are any changes in the gate inter-residue distances. This loosening of the protein even before the gate opens might be a part of the enthalpy−entropy balance that accompanies the ligand's passage through the protein. Our results provide an energy profile of the ligand during its entry/exit into/from the protein and can, in principle, enable one to assess the residence time, which in turn may be associated or indirectly correlated with adverse cardiovascular side effects of nonsteroidal anti-inflammatory drugs. We believe that similar analyses for other selected COX-2-specific inhibitors will provide a measure (or prediction) of possible toxicity effects.

INTRODUCTION

Nonsteroidal anti-inflammatory drugs (NSAIDs) have been widely used to treat pain, fever, and inflammation.[1,2] The principal pharmacological effect of NSAIDs is well-established, and their inhibitory activity on both forms of cyclooxygenases (COX-1 and COX-2) is also well-studied. Some COX-2 selective inhibitors on the market have been associated with adverse cardiovascular side effects, leading to recent restrictions on their marketing. The physiology and pathophysiology of COX continues, therefore, to be a matter of great interest.[3−7] Chart 1 shows some COX-2 selective inhibitors and SC-558, which is the subject of the present study.

Relative binding affinities of selective and nonselective COX-2 inhibitors have been studied previously by docking, Monte Carlo simulations, and molecular dynamics (MD) methods.[10−13] The active site in COX is situated deep in the protein; to reach it, the ligand has to travel from the exterior to a shallow cavity which then leads to the active site across a narrow opening called the gate. It is believed that the residues Arg120, Tyr355, Arg513, and His90 constitute this cavity/gate region (Figure 1).[12,14] Kinetic studies have been performed to correlate the potency of selective and nonselective inhibitors with free energies and to establish the nature of ligand−protein interactions, in terms of slow-binding, tight-binding, and reversible inhibition.[15] It is believed that slow-binding inhibitors undergo large-scale conformational changes when they enter or leave the active site. Structural features that can account for time-dependent inhibition as in the case of many COX-2 selective inhibitors are dynamic rather than static, and conformational changes in the ligand are probably involved in the entry and exit.[16]

It has been noted that rates of association and dissociation of the protein and ligand differ, the former being faster. Marnett et al. have studied the association and dissociation

* Corresponding author (G.R.D.) tel.: 91-40-23134828; fax: 91-40-23010567; e-mail: gautam_desiraju@yahoo.com; (J.A.R.P.S.) tel: 91-40-55259990; fax: 91-40-55626885; e-mail: sarma@gvkbio.com.
[†] School of Chemistry, University of Hyderabad.
[‡] Informatics Division, GVK Biosciences Pvt. Ltd.

10.1021/ci050142i CCC: $33.50
Published on Web 05/09/2006

Chart 1

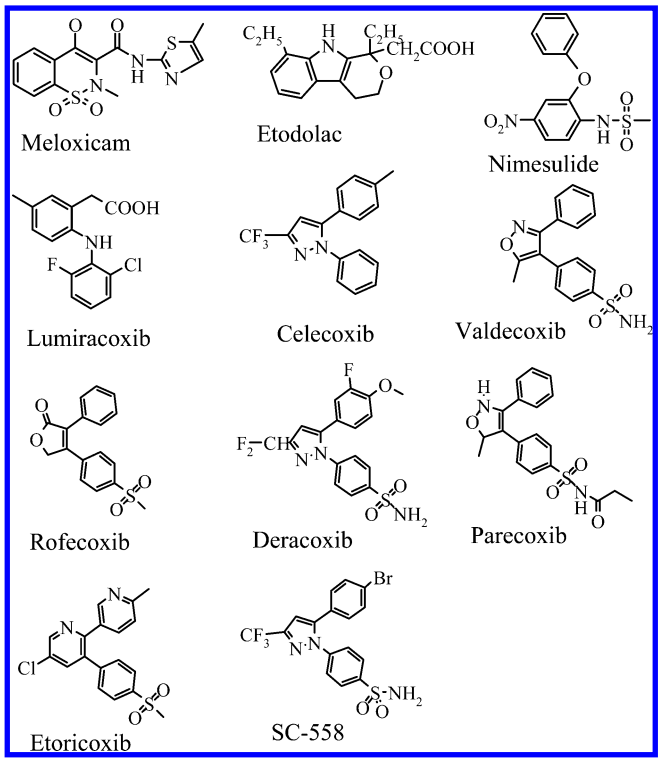

of SC-299, a close analogue of SC-558, with COX-1 and COX-2 and have shown that, while association of the ligand to the COX-2 active site takes only around 30 s, dissociation takes about 3−4 h.[15] Accordingly, and in order to understand the process of exit and entry of the ligand from the active site to the protein surface, and to assess it at a structural level, we have performed a *ligand coordinate analysis* wherein the ligand SC-558 is dissociated from the active site of the COX-2 protein in several sequential steps and moved to the protein exterior using MD techniques at each step.

There has been a report on ligand binding and unbinding using steered molecular dynamics simulations that mimic the principles of atomic force microscopy.[17] Another study reports ligand docking along a smooth association pathway.[18] Vetrivel and Deka have modeled a sorbent molecule which was constrained and minimized in a number of locations along a mean predefined path in a zeolite to understand its diffusion profile.[19] We have adopted a similar methodology in a protein environment. Our study aims to provide an insight into the intermolecular interactions formed by the ligand as it moves from the active site to the outside.

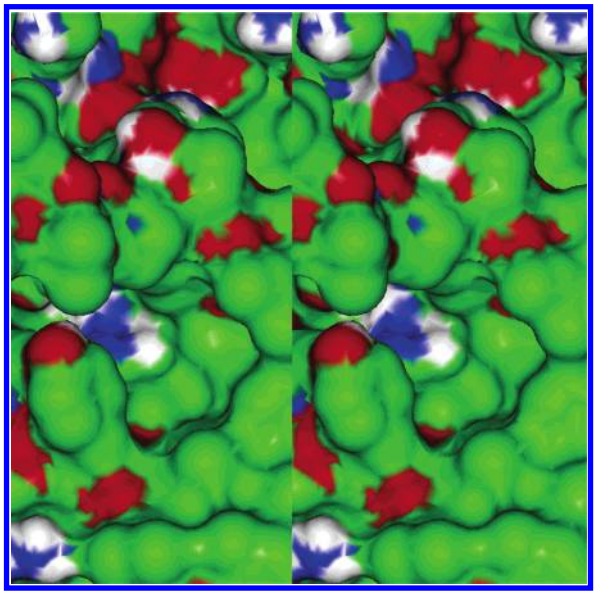

Figure 1. Stereoview of the electrostatic map of the COX-2 surface to show the cavity. Note the important Arg120 residue in the center (blue surrounded by white).

METHODS AND MATERIALS

Enzyme Preparation. The published crystal structure of COX-2 with SC-558 as the ligand in the active site (1cx2) was taken for the ligand coordinate analysis. Only one monomer (with 556 residues) of the tetrameric protein was considered. The H atoms were fixed using standard protocols. The active site was defined as consisting of all residues (excluding the heme part of the protein) with at least one atom within a distance of 10 Å from any atom of the ligand. The active site was hydrated using the Soak module of MOE with a layer width of 1 unit. This resulted in the addition of 160 water molecules—a few in the active site and most of them on the surface of the protein. The residues in the active site, ligand, and all water molecules were subjected to minimization and dynamics studies, while the rest of the protein (including the heme part) was fixed. The His residues 90, 95, 351, 356, and 386 were designated as the ϵ tautomers.[20] The residues Arg, Glu, and Asp were taken in their ionic form. All minimization and dynamics calculations were carried out on a Silicon Graphics Octane2 R12000 computer using the CCG/MOE software.[21] Minimization after the MD study and further analysis was carried out with Cerius[2] using the CVFF force field and the default charges, while electrostatic map figures were produced with Insight II.[22,23] The AMBER force field was used in MOE along with the assigned atomic charges. Distance-dependent dielectric constants were used in the evaluation of electrostatic forces.

CVFF and AMBER are class I force fields, and they are unlike the more specific and customized class II force fields, for example, Dreiding and CFF95. However, we are attempting to evaluate the broad statistical picture here rather than individual specific geometries, and CVFF and AMBER, which are the most commonly used force fields in the modeling of macromolecular systems, are preferred for reasons of generality. Further, any MD study produces average conformations and energies; the subtle effects of the particular force field chosen may be considered as being of secondary importance.

In the ligand coordinate analysis, the SC-558 molecule was moved incrementally from the active site to the surface (Figures 2 and 3). The midpoint of the N1−C5 bond was defined as the reference point for the ligand, and its location in the active site was considered as the starting point of the path (point A). The midpoint of the intermolecular vector defined by the Nη atom of Arg120 and the Oη atom of Tyr355 (gate residues) in the crystal structure was next defined as point M. The vector **AM** was extended to a distance of 17.52 Å, and the point thereby defined is X, which is the end point of the ligand trajectory. This point is well outside the protein (Figure 2). The actual path covered by the ligand between points A and X should ideally be based on the local minima of a multiwell potential energy surface.

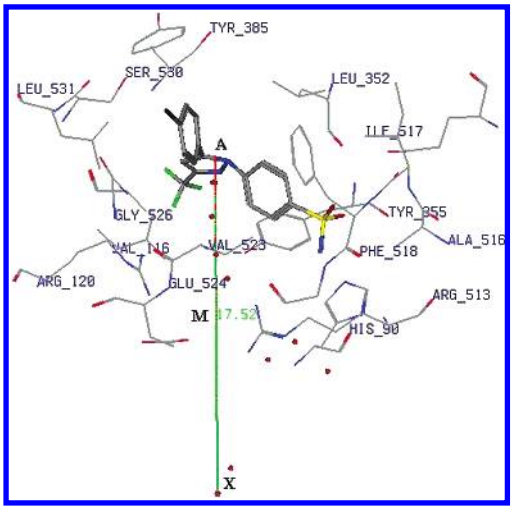

Figure 2. Definition of ligand trajectory AMX. The point M is defined as the midpoint between Cζ of Arg120 and Oη of Tyr355, which are located at the gate. Red dots indicate the actual points of ligand movement along the path (see Figure 3). AX = 17.52 Å.

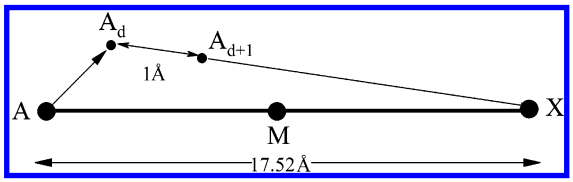

Figure 3. Movement of the ligand between lowest-energy minimized positions, A_d. The ligand is moved in the direction of the $\mathbf{A_dX}$ vector by a distance of either 1 or 2 Å.

A good approximation to this path is obtained with the following procedure. The ligand at point A was minimized and subjected to the MD run as described below. Let us suppose that the ligand has moved to point A_d (Figure 3). For the next MD run, the ligand is moved a distance of 1.0 or 2.0 Å along the vector defined by the points A_d and X. The new position of the ligand thus obtained is the point A_{d+1}. The next MD run is carried out at this location, and the procedure repeated until the ligand eventually reaches the region of point X. In all, 13 points were thus generated, at distances of 0.0, 0.9, 1.2, 1.8, 3.6, 5.8, 8.2, 10.0, 10.5, 12.5, 12.7, 17.0, and 17.52 Å from the active site, and these points define the *ligand path* from A to X, in other words, the progress of the ligand through the protein. For each point, A_d, on the path, minimization and dynamics calculations were performed as follows. For minimization, the system was treated in multiple steps: (1) water alone varying, (2) the ligand and water varying together, (3) the side chains, ligand, and water varying together, (4) the backbone, ligand, and water varying together with the side chains fixed, and (5) the complete protein, ligand, and water varying. At each step, 10 000 iterations by steepest descent methods followed by conjugate gradient methods were carried out. After a successful (that is, uneventful) minimization wherein the gradient is below 0.01 kcal mol^{-1} or the change in the gradient is less than 0.001 in three successive iterations, the system was subjected to a dynamics run. Upon moving the ligand to each new point on the path, the water solvation was redefined, and all residues within a 10 Å distance from any atom of the ligand were included in the corresponding dynamics run. To keep the energy book keeping intact, the number of water molecules was kept constant (at exactly 160) during each of these 13 runs. For each minimization/dynamics run, a distance restraint was applied to the ligand with a weight of 9, such that it would not move back to its initial location (point A) but would, however, find a regional/local minimum within, say, a 1 Å radius sphere of the prevailing position without any unreasonable increase in energy.[24] The passage of the ligand from A to X represents, effectively, a ligand coordinate analysis.

MD calculations were carried out initially by heating the minimized structures to 300 K at a constant rate of 100 K/ps followed by a 100 ps equilibration. A further 250 ps dynamics run was saved at regular intervals of 1 ps for analysis (total of 250 conformations). The time step was set to 1 fs, and a cutoff of 7.5 Å was used to compute nonbonded interactions. The total time of the simulations is therefore ~5 ns. The total energy, potential energy, and enthalpy were saved during each MD run. One of the lowest-energy conformations (of the 250) was further minimized (preferably at the end of the MD run); this geometry was taken as the input for the minimization/dynamics at the next point on the path. We noted that the positioning of the ligand at or near point X (17.52 Å) was difficult and that the molecule essentially escaped into a vacuum in such a situation. Unlike in the zeolite studies of Vetrivel and Deka,[19] we applied restraints at each point followed by minimization and MD runs. This was done so as to identify all possible local minima in the vicinity, so that the trajectory of the ligand could be well identified.

For each MD run, two measures of the ligand and protein structure were taken. In the first instance, an average structure was obtained from the above-mentioned 250 conformations and minimized. Alternatively, the 10 lowest-energy conformations of the 250 were selected and individually minimized. We believe that the 10 lowest-energy conformations provide finer details on the consistency of specific and strong interactions and also the geometries of the ligand and the amino acid residues around the ligand. Some of these distances are given in the Supporting Information, where they have been compared with those from the average structure. From the aforementioned 10 structures, one was identified as representative, and this is used for further discussion. Figure 4 shows the potential energy profile across the 13 points in the ligand path. Figure 5 gives the potential energy for the average structure at each of the 13 points. Figure 6 is a residue-wise (Figure 6a) and water-wise (Figure 6b) representation of short intermolecular contacts to the ligand at each point in its path. Table 1 gives intermolecular distances, less than 2.6 Å, between the ligand and various residues and water molecules in the active site selected from different frames of the MD run. The geometries obtained in each run were minimized before inclusion in this table. Similar distances from the average structure are also given. For similar interaction data for the other points on the path, see the Supporting Information.

An important question concerns the reproducibility of the ligand path in independent computer experiments. Given the expected large number of local energy minima over such a long binding pathway, the minor force field inaccuracies, and the need to add constraints to get the system to cover the chosen path, would the same path be replicated over two or more runs? Also, would such a pathway also be reversible? In this context, it may be stated that MD is an averaging type of technique; the simulation was carried out for a

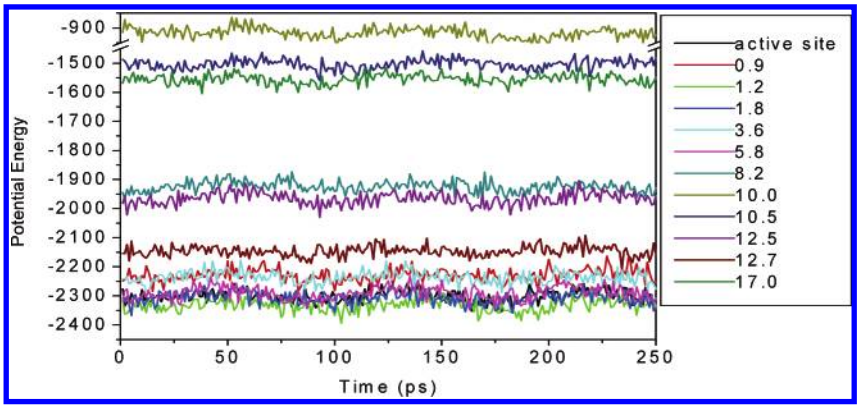

Figure 4. Variation in the potential energy for each MD run. Note that the potential energy is fairly stable in each run, indicating the system is well-behaved during the MD run.

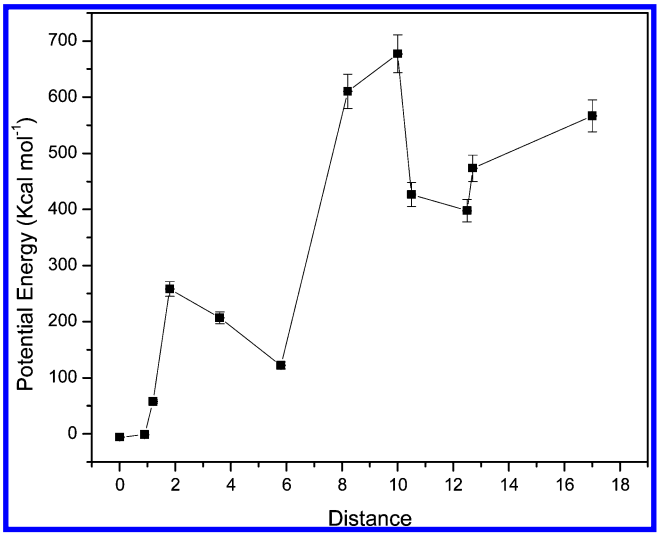

Figure 5. Variation of potential energies (with error bars) after minimization with the distance of the ligand from the active site to outside the protein. Notice the cavity between 10 and 12 Å. The energy maximum at ~10 Å represents movement of the ligand through the gate.

sufficiently long time (until a very good equilibration was achieved) and the precaution taken of considering the 10 lowest-energy frames for each distance. The energy differences between these frames are also very small. The distance between any two successive points is also manageably small (ca. 1.0 Å). We conclude, therefore, that nearly the same pathway would be obtained in independent runs and that the differences between these pathways will not alter our major conclusions.

RESULTS

The passage of the ligand through the gate has been discussed previously for COX-2 selective inhibitors.[10,12] It is believed that there is a cavity just before the gate and that the ligand is bound reversibly in this cavity before entering the protein proper.[14] It has been suggested that the ability of the ligand to perturb the hydrogen-bond network between the gate residues Arg120, Tyr355, and Arg513 determines the kinetics of its entry and exit.[12] From the outside, the cavity is the first binding site. It is believed that the binding of both selective and nonselective ligands is reversible in this site, in other words, time-independent.[14,15] The second binding site is the active site itself, and the ligand must clear an activation barrier to move from the first binding site (cavity) to the second binding site (active site). Binding at the second site is different for selective and nonselective inhibitors: while nonselective inhibitors (indomethacin and profens) bind reversibly, selective inhibitors (SC-558 and coxibs) bind irreversibly, that is, in a time-dependent manner. This MD study is intended to better our understanding of the gating mechanism, the nature of the recognition at these multiple binding sites, and the activation barrier between the binding sites. Our analysis involves the ligand movement between 13 points from the active site to the protein exterior. This would correspond to the exit of the ligand from the protein. We assume that ligand entry would be the reverse process. [15]

Also important is the effect of water molecules. There is overwhelming evidence that hydrogen-bonded networks involving water are crucial for the ligand to enter into the active site. The following results are relevant: (1) COX is located in the lumen of the nuclear envelope and endoplasmic reticulum,[25] and (2) the membrane binding domain of COX-2 is amphipathic and forms an entrance to a long hydrophobic channel.[26] Because of this amphipathic entrance, there is every chance that water may get inside the protein. Selinsky et al. have mentioned that some (structural) water may assist in maintaining the native structure of the enzyme even in the absence of a substrate.[27] They go on to say that there is a narrow solvent channel that branches off from the top of the COX channel which is connected to the outside of the protein by a narrow solvent channel. This channel serves as a safety valve allowing water to escape from the top of the COX active site as a substrate enters from the bottom. Pouplana et al. have stated clearly that "well ordered water molecules can be identified in the COX channels... these waters are seen in all structures and appear to play key roles in maintaining the structural integrity of the channel. Molecular modeling studies performed on the two isozymes suggest that active site hydration is also crucial for the selectivity of ketoprofen analogs."[28]

Figure 4 shows that, within a particular MD run, the potential energy is very stable and is not associated with large fluctuations. This confirms the reliability of the computations. However, there are wide variations between runs, and this is indicative of chemical changes along the path (Figure 5). The much lower energy at the active site relative to the protein exterior is indicative of an overall thermodynamic impetus to binding. Put another way, it is easier for the ligand to enter the protein than to leave it.

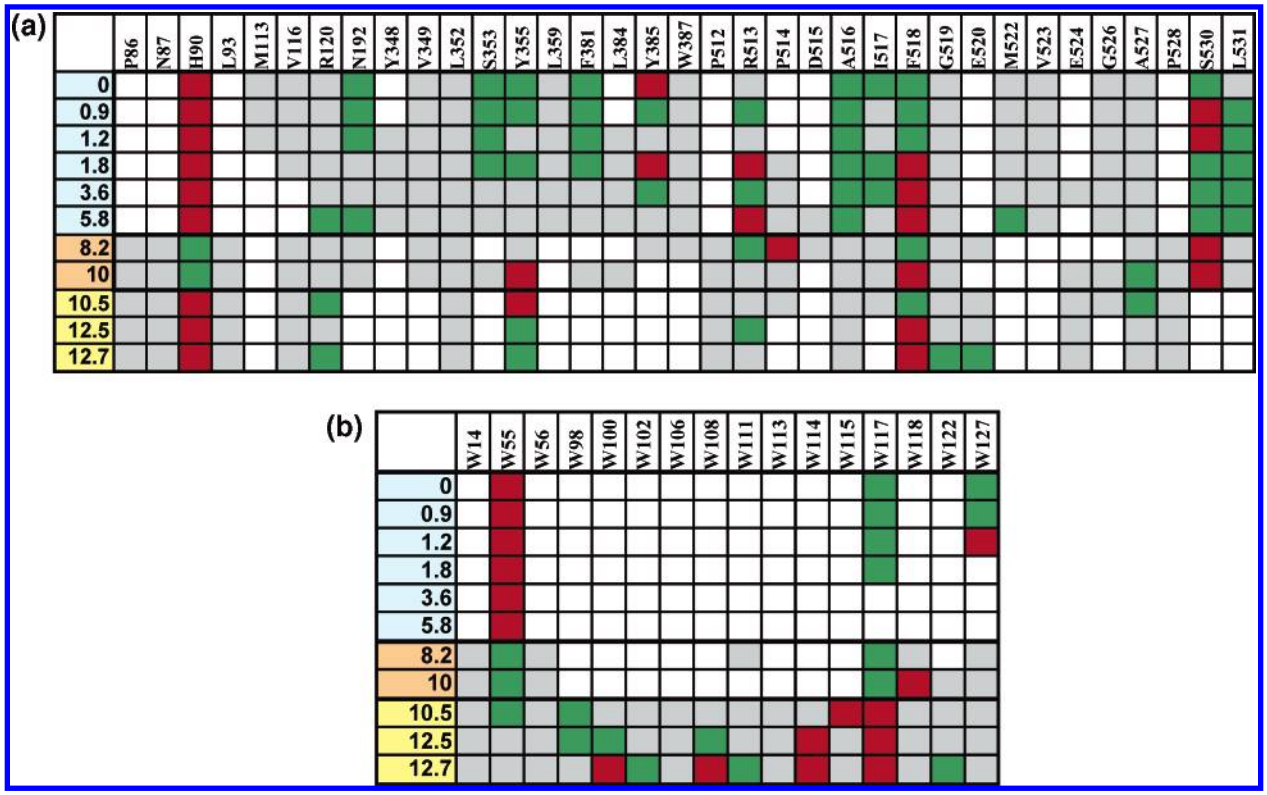

Figure 6. (a) Three stages of SC-558 movement from the active site to the surface of COX-2. Residues within 4 Å from any atom of the ligand are shown in gray. Residues that do not appear within the 4 Å sphere are shown in white. Residues within the van der Waals interacting distance are shown in green. Residues that form strong hydrogen-bond interactions are shown in red. The three stages of ligand movement are shown in cyan, orange, and yellow. Some residues within the 4 Å sphere do not appear in the later stages and vice versa. Some residues such as His90, Tyr355, Arg513, and Phe518 form strong interactions all the time. Arg120, Leu352, Ala516, Gly519, and Ala527 are within 4 Å from the ligand nearly always. (b) Matrix for water−ligand interactions. W55 forms strong interactions with the SO_2NH_2 group of the ligand in the first stage (cyan), weakening in the later stages. W117 forms strong hydrogen bonds in the third stage, and the importance of water−ligand interactions, in general, in the third state is apparent.

Table 1. Inter Ligand−Residue and Ligand−Water Distances (Å) in the 10 Minimized Structures and the Average Structure of the MD Run at the Point $A_d = 0.0$ (Active Site)

	interaction ligand−residue	54	98	130	151	163	202	214	233	289	300	av.
1	SO_2.....HN (His90)			**1.8**		1.9				2.2	2.4	2.2
2	HN.....HN (His90)							1.9				
3	SO_2.....HOH (55)	2.31	2.1	**2.4**	2.0		2.1	2.5	1.9	2.0	2.2	2.2
4	SO_1.....HN (Gln192)		2.6	**2.6**								
5	NH.....O═C (Phe518)			**2.1**	2.6					2.2	2.4	
6	SO_2.....HC (Ser353)			**2.6**			2.6	2.4	2.5	2.6		
7	SO_1.....HC (Ile517)			**2.6**	2.3							
8	SO_1.....HN (Ile517)				2.3						2.1	
9	SO_1.....HC (Ala516)						2.4	2.5	2.4	2.5	2.4	2.5
10	Br.....HO (Tyr385)		2.5	**2.5**		2.3		2.3	2.6			2.4
11	Br.....HO (Ser530)		2.5	**2.5**								
12	bromophenyl H.....OH (Ser530)	2.56	2.5	**2.5**	2.4	2.5	2.4	2.4	2.5	2.4	2.3	2.4
13	bromophenyl H.....HOH (127)	2.48	2.3		2.5		2.3	2.3		2.3	2.3	
14	sulfonamide H.....OH (Tyr355)				2.3							
15	$CF_{3(2)}$.....HOH (117)			**1.9**								2.2
16	$CF_{3(2)}$.....HC (Leu359)			**2.5**								
17	$CF_{3(3)}$.....HOH (117)					2.1			2.3			
18	$CF_{3(1)}$.....HC (Leu359)									2.5		

The low energy barrier at 1.8 Å perhaps corresponds to the loosening of the sulfonamide group from the deep pocket. The energy rises sharply to a maximum at 10.0 Å, indicating that the passage of the ligand from the protein interior to the cavity is hindered. The local minimum between 10.5 and 12.7 Å is clear evidence for the cavity. Subsequent movement to the exterior is easy and is in keeping with the idea that binding in the cavity is reversible. Entry and exit of the ligand into the protein is, therefore, a two to three step process, as also indicated by kinetic studies.

Figure 6a is a color-coded representation of short contacts between the ligand and protein during the path from A to X. Red squares signify that the residue in question forms one or more strong NH···O and OH···O hydrogen bonds to the ligand.[29] Green squares represent contacts (other than the above) shorter than van der Waals separation. Grey squares represent residues that are situated at a distance of up to 4.0 Å from the ligand. Blank squares cover all of the

remaining residues and are neglected in the analysis of nonbonded contacts. The following observations and inferences may be drawn: (1) As the ligand moves through the protein, contacts with some residues become weaker while contacts with others get fortified, so that a particular residue assumes significance at different points on the ligand pathway. For example, Trp387 is within a 4.0 Å distance of the ligand until the 8.2 Å point and then fades out. Again, Ser530 and Lys531 are strongly bound to the ligand until the 10.0 Å point but drop out after that. Accordingly, one obtains a more definite picture of the ligand path through the protein. (2) Some residues are always in contact with the ligand, although the specific interactions might vary. Typical examples are His90, Arg120, Tyr355, Arg513, and Phe518. Significantly, four of these residues are associated with the gate and cavity. Such residues, which are always in contact with the ligand, represent hinge or pivot points in its passage through the protein. Other residues such as Lys352, Gly519, and Ala527 are continuously close to the ligand, but they do not have specific interactions. (3) A closer inspection of the squares reveals that there are three distinct *stages* in the progress of SC-558 from A to X. The first of these covers the region between the active site and the point at 5.8 Å. The second covers the short distance between 8.2 and 10.0 Å. Significantly, stage 2 is associated with maximum energy and structural instability. The third stage covers the distance between 10.5 Å and the exterior. This demarcation into stages is justified by the respective interaction patterns. There are many interaction discontinuities, that is, color changes (red to green, green to red, and green to gray), at the transitions between 5.8 and 8.2 Å and also between 10.0 and 10.5 Å. Figures 4 and 5 show that these interaction discontinuities are also accompanied by concomitant energetic and conformational discontinuities. Therefore, these stages have chemical and dynamic significance. Figure 6b is the corresponding interaction matrix for contacts between water and the ligand. The distinctions between stages 1 and 2 and between stages 2 and 3 are shown nicely by W55 and W117. The interaction patterns of other water molecules are also in accord with this demarcation into stages. As the ligand nears the protein surface, it is surrounded by more water molecules; this is to be expected. The typical interaction patterns in each of the stages are shown in a cartoon depiction in Figure 7a−c. The Supporting Information contains an animated sequence of 120 frames (10 minima in each of the 12 runs) and gives a good idea of the actual movement of the ligand. The discontinuities between the stages are easily noticeable in this "movie" of the ligand journey. A panel of illustrations in Figure 8 shows the ligand conformation and orientation at each of the 13 points and provides an abbreviated version of the movie.

Stage 1. This stage consists of 6 points and involves subtle conformation, orientation, and translation changes of the ligand in and near the active site. During the movement of the ligand between 0.0 and 5.8 Å, the O1 atom of the SO_2-NH_2 group is involved in hydrogen bonds with the NH of Phe518 and the CH of Ala516. The O2 atom is hydrogen-bonded to the NH of His90 and the OH of W55 (Table 1). His90 also donates to the sulfonamide N atom. Also important are NH···O bonds from the ligand to backbone carbonyl O atoms of Phe518 and Arg513. The Br atom of the ligand forms Br···H−O interactions with Ser530 and

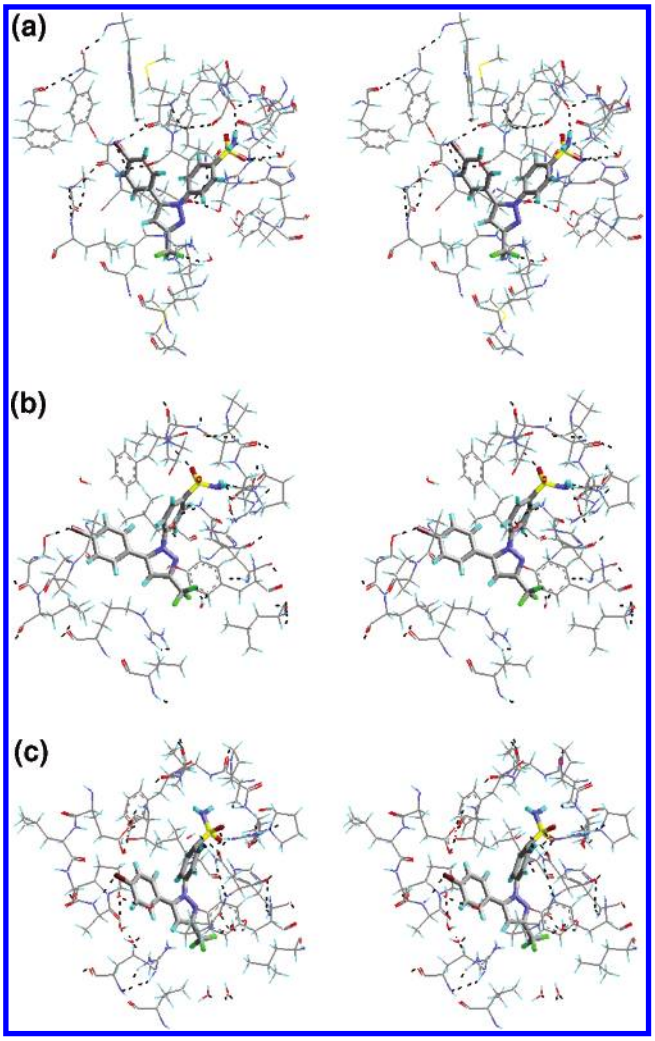

Figure 7. (a) Representative view of SC-558 in stage 1, showing all residues and water molecules within a 4 Å radius around any atom of the ligand. Inter-residue, protein−ligand, ligand−water, and water−residue hydrogen bonds are indicated with dashed lines. This illustration is one of the minimized structures from the MD run for the point $A_d = 0.0$ Å (active site). (b) Representative view of SC-558 in stage 2 at the point 8.2 Å. (c) Representative view of SC-558 in stage 3. Notice the water−ligand interactions.

Tyr385, while aromatic CH groups in the bromophenyl rings form CH···O interactions with W127. Some good CH···O bonds are also observed from Ser353 to O2 of the sulfonamide group and from Ala516 and Ile517 to O1. Notably, the CF_3 group of the ligand interacts with W117 and the CH groups of Leu359 and Leu531. While the primary role of the CF_3 group might, in general, be to enhance the acidity of the adjacent C−H groups toward hydrogen bonding, other implications of "organic" fluorine such as their acceptor capability in hydrogen bonding cannot be ignored (Table 1).[30,31] This substituent seems to be important in ligand−protein recognition.[32,33] The Supporting Information gives details of the interactions at all points on the ligand path. To summarize, stage 1 consists of various conformational changes of the two phenyl rings of the SC-558 ligand even as the sulfonamide group is firmly installed in the deep pocket of COX-2. There is a slight loosening of the bromophenyl ring toward the end of this stage. Energy changes during this stage are not substantial. A characteristic feature of the ligand movement (in this and, for that matter, the two other stages also) is that the interactions between

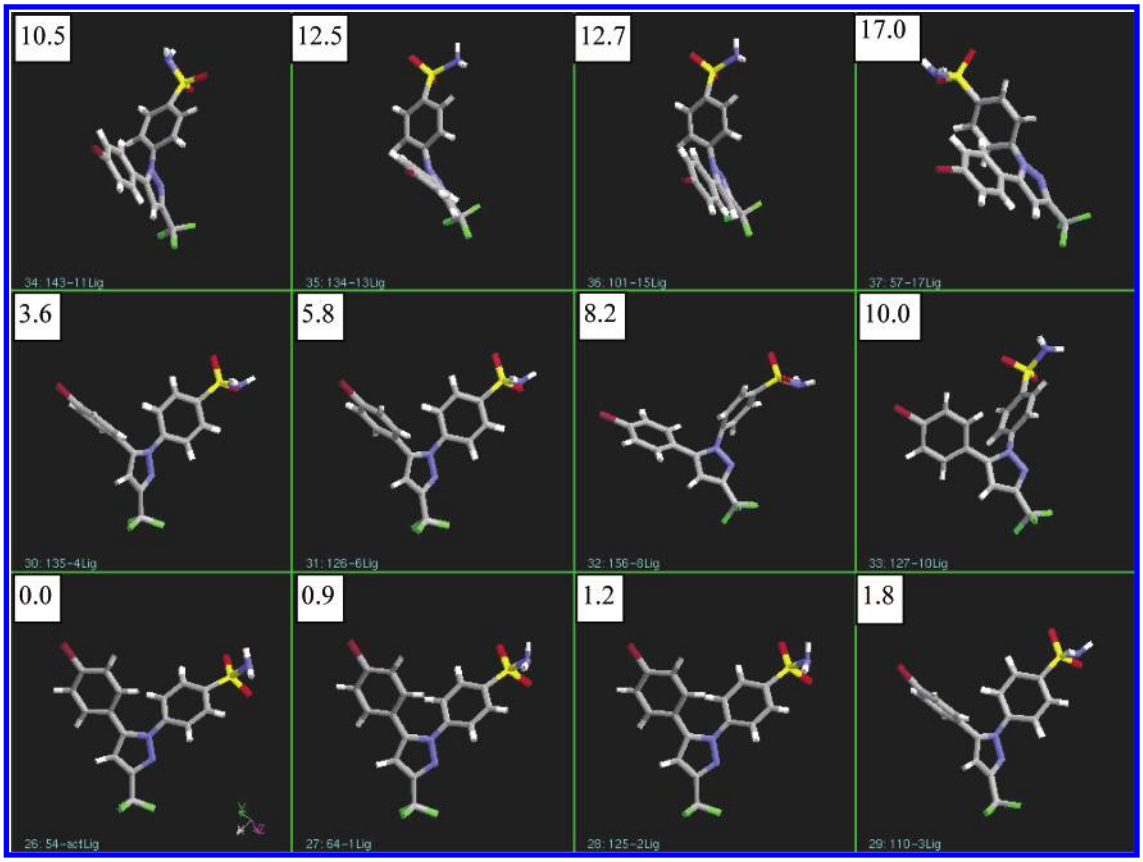

Figure 8. Conformational and orientation changes of SC-558 at different points along its path. Distances, A_d, from the active site are indicated. See Figures 2 and 3 for the path definition. Notice the discontinuities around 8.2 and 10.5 Å. All of the illustrations are from the same view with respect to the protein.

the ligand and the protein are broken and made in a relaylike fashion. This is illustrated in Figure 9 with details in the Supporting Information. Notably, there are many instances of bifurcated (or anticooperative) hydrogen-bond schemes that are necessary for this relaylike pattern. Anticooperative hydrogen-bond schemes are not common in small molecule crystal structures. They are far more common in macromolecular structures, and the implication is that their role is functional rather than purely structural.

Stage 2. This is the critical stage in the ligand pathway, especially at the 8.2 Å distance. This stage corresponds to the maximum energy level of the system. The ligand swivels around 45° about an axis roughly perpendicular to the pyrazole ring without much disturbance of the sulfonamide group in the deep pocket. In contrast to stage 1, the bromophenyl ring is now coplanar with the pyrazole ring, while the sulfonamide ring is nearly perpendicular (Figure 7b). Rotation around the C−S bond occurs so that hydrogen bonds accepted by O1 are now accepted by O2. In stage 1, there was a smooth transition between the various hydrogen bonds. Figure 9 shows that in stage 2 there is an abrupt change in the hydrogen-bond patterns. A number of new residues and more water molecules surround the ligand (Figure 6a,b). All in all, there are fewer ligand−protein interactions in this stage (accounting, in part, for the higher energy), and the ligand seems to be moving toward a (supramolecular) transition state wherein the sulfonamide group leaves the deep pocket, and the CF_3 group is now positioned near the gate as a prelude to its imminent exit.

Figure 8 shows snapshots of the ligand at the various points along the ligand coordinate trajectory. The snapshot at 8.2 Å shows a ligand in a distorted geometry, with what appears to be a substantial bending of the C−N bond at the center of the ligand and the C−S bond in the sulfonamide fragment. This coincides with the point at which the minimization energy increases, allowing the conclusion that there is an energy barrier here. An important concern is how much of this energy barrier can be ascribed to the unusual ligand geometry. Is the potential energy map in Figure 5 an artifact of unreasonable changes in ligand geometry, which the force field allows to happen? In response, one could say that there is indeed a distortion of the ligand at the 8.2 Å position but that this occurs because the ligand has a real problem in going through this narrowest part of the pathway. Further, boat-shaped geometries for aromatic systems are not unusual in themselves, especially when strain is involved, and a good example of bending of C−N and C−S bonds in the same sense is provided by the boat-shaped molecule *p*-(trimethylammonio)benzene sulfonate.[34] We have also stated earlier in this paper that the effects of the force field are minimal in these statistical approaches. The magnitude of the energy barrier may not be the most accurate, but what is important is that the ligand distortion occurs *only* at the 8.2 Å position. The protein and the ligand behave properly in the other positions, and we are reasonably confident about relative energy changes in these other positions along the pathway. Finally, if the force field were inappropriate, the protein itself would collapse and the ligand would not stay at the preset positions, during the long MD simulations of the type we report. To summarize, we feel our results are not artifacts of the computation. Accordingly, we believe

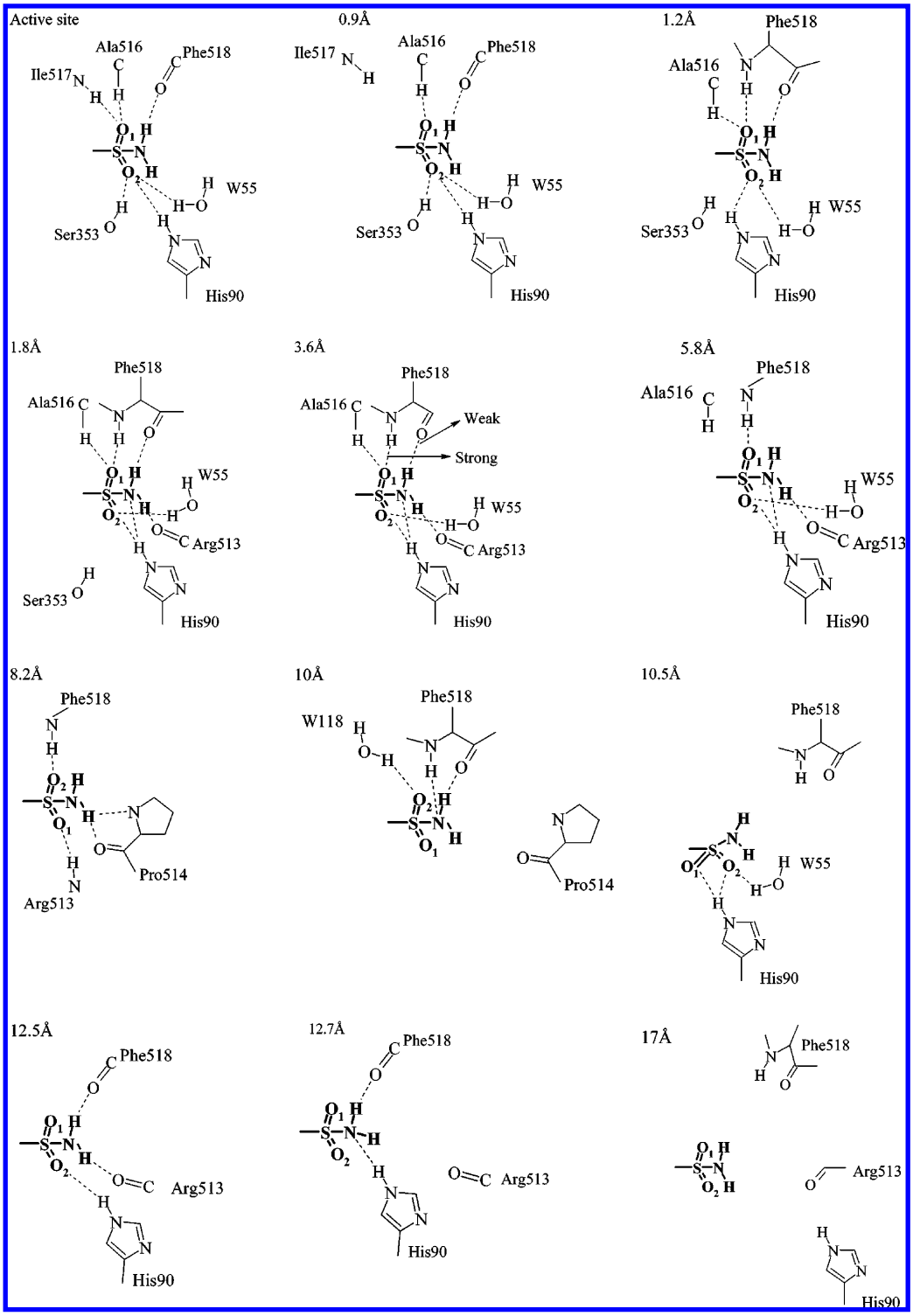

Figure 9. Strong and weak hydrogen bonds formed by the sulfonamide group of SC-558 with different residues in various points. Notice the anticooperative hydrogen bonds formed by the ligand as it moves from one point to another along its path.

that the distortion of the ligand at this point is chemically significant.

Stage 3. This stage involves the movement of the ligand through the gate to the exterior. To do this, the ligand must undergo an orientational change as illustrated in Figure 7c. During this stage, the ligand is involved in translational motion toward the exit. Both sulfonamide O atoms are involved in bifurcated H bonds with the NH of the His90 imidazole ring. N2 of the pyrazole ring is involved in interactions with W115 and Tyr355. Toward the later points in the path, the ligand is surrounded by several water molecules in a manner reminiscent of the clathrate hydrates:[35] it would appear that the ligand needs this hydrophilic vehicle to transport it out of the hydrophobic protein interior (Figure 7c). During the opening of the gate, Arg120 rotates completely inward and forms a hydrogen bond with a backbone N atom while the other NH group is bound to water. At the 17 Å point, the ligand sits well in the cavity (Figure 10). This is at the very end of the path, and it was observed that, when the lowest-energy conformations of the MD run were minimized, the ligand moved slightly to the inside; in other words, there is a small driving force for it to

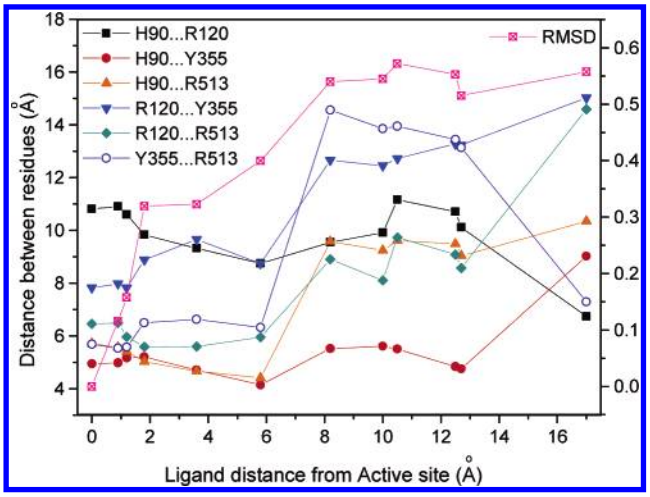

Figure 10. Distances between important residues surrounding the ligand and the RMSD of the entire protein as a function of the ligand distance from the active site. Notice the variation is highest for those distances involving Arg513 (second gate) residues and between Arg120 and Tyr355 (first gate) residues. Note that the increase in RMSD occurs well before the inter-residue distances start to vary, indicating that the protein loosens up as soon as the ligand begins to move.

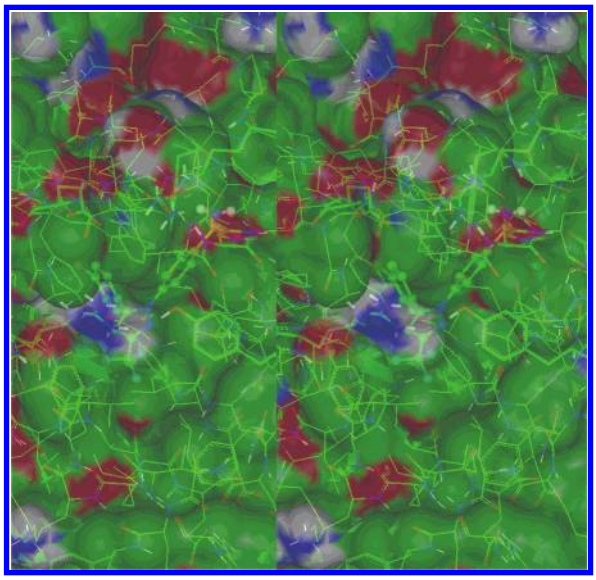

Figure 11. Electrostatic potential surface map with partial transparency showing the cavity, ligand (ball-and-stick) in the active site, and some residues (Figure 1). The Arg120 and Tyr355 residues (first gate) are in front of the ligand, while the Arg513 and His90 (second gate) residues are near the sulfonamide group. These gate residues are shown in stick mode.

remain in the cavity, which is a true energy minimum (Figures 5 and 10). If the ligand is moved further outside, it moves very far away from the protein (>50 Å) and the 160 water molecules end up on the protein surface. This is the end of the simulation.

Entry, Exit, and Half-Life of the Ligand. The MD simulations provide a realistic picture of the molecular- and supramolecular-level processes that take place during the entry or exit of the ligand into or from the protein. But, what about the cavity and the gate? Figure 10 is a plot of inter-residue distances in the gate/cavity region versus the ligand position in the protein, and Figure 11 is the electrostatic potential surface showing the cavity, ligand, and surrounding residues. The gate consists of an opening created by the junction of Arg120 and Tyr355 and also the opening between Arg513 and His90; in a sense, there are two gates, and the second one controls the entry and exit of the ligand from the deep pocket, while the first is necessary for the ligand to move into the cavity from the interior. The Arg513 residue is the most crucial for the gating mechanism. Either its movement facilitates the ligand exit from the deep pocket or it is dragged along continuously with the ligand during its exit because of strong hydrogen bonds. Similarly, Phe518 and His90 also play a crucial role for ligand exit from the deep pocket and, to a lesser extent, so does the opening between Arg120 and Tyr355. Figure 10 shows the maximum energy increase in the gate opening process when the ligand is between the points at 5.8 and 12.7 Å. The figure also provides good evidence for the presence of the cavity. All of the distances become slightly smaller as the ligand settles into the cavity, and the protein, in a sense, "tightens". Most interestingly, however, the variation of the root-mean-square deviation (RMSD; of all residues) begins to increase almost as soon as the ligand leaves the active site (0.0 Å), *although no major changes in the gate inter-residue distances are apparent until the 5.8 Å point.* This gives the compelling feeling that the protein as a whole "loosens up" immediately as the ligand leaves the binding site; in a sense, this loosening is a prelude to the gate opening that will occur in a little while. One might say that this loosening is a part of the enthalpy−entropy balance[36] that accompanies the ligand's passage through the protein. The reader will note that entropic considerations are of the greatest significance during the ligand's passage; in a macromolecular environment, the loss of intermolecular interactions is compensated by the overall movement and loosening of the protein, in effect, an increase in entropy.[37]

Table 2 shows a comparison of the plasma half-life values ($t_{1/2}$) for a number of selective and nonselective COX-2 NSAIDs.[38] Most of the selective inhibitors have longer $t_{1/2}$ values, and in general, efforts are made to design drugs with longer $t_{1/2}$ values for higher efficacies with minimum dosages. The nonselective inhibitors may have small or large $t_{1/2}$ values (ibuprofen and piroxicam). However, it has been stated that longer $t_{1/2}$ values may be associated with toxicity.[39] In the present context, we note that, whether the inhibitor is selective or not, a long $t_{1/2}$ is always associated with adverse cardiovascular side effects (rofecoxib and piroxicam). Notwithstanding metabolism, elimination, and other related issues, these observations show that the adverse side effects of some COX-2 selective inhibitors might be a consequence of their longer $t_{1/2}$ values because their continued activity for longer time periods could cause a greater imbalance between the prostanoids, namely, prostacyclin (PGI_2) and thromboxane A_2 (TXA_2).[40] Fluorescence quenching experiments on the dissociation kinetics of SC-299, which is a close analogue of valdecoxib, have shown that the ligand takes hours to dissociate from COX-2 in contrast to its ~30 s dissociation time from COX-1.[12] Our present results provide an energy profile of the SC-558 ligand during its entry/exit into/from the COX-2 protein. We believe that similar analyses for other selected COX-2 specific inhibitors will provide a measure (or prediction) of residence times and, accordingly, of possible toxicity effects. There are many advantages in having COX-2 specificity: optimally, one would like to balance these with a minimum residence time

Table 2. Plasma Half-Life Values ($t_{1/2}$) for Some Nonselective and COX-2 Selective NSAIDs[a]

nonselective NSAIDs	plasma half-life (H)	selective NSAIDs	plasma half-life (H)
Compounds with Relatively Lower $t_{1/2}$ (<6.0 h)			
diclofenac potassium	1−2		
flurbiprofen	5.5		
ibuprofen	2.0		
indomethacin	2.4		
ketoprofen	1.8		
ketorolac	5.3		
mefenamic acid	2−4		
salicylic acid[b]	1.71		
Compounds with Higher $t_{1/2}$ (= 6.0 h)			
carprofen	9.4	celecoxib	11−13
fenbrufen	10−17	cimicoxib	17−26
meloxicam	15−20	etoricoxib	21.7−22.5
piroxicam	48	rofecoxib	17
		tilmacoxib	44.5
		valdecoxib[c]	8−11
		deracoxib	10.5[d]
		lumaricoxib	3−6

[a] Nonselective NSAIDs have a wide variation in $t_{1/2}$ values, while most of the COX-2 selective NSAIDs have higher $t_{1/2}$ values. NSAIDs with lower $t_{1/2}$ values are, in general, less associated with adverse cardiovascular side effects. [b] Aspirin has a half-life of 0.25−0.33 h and is a nonreversible NSAID. [c] Parecoxib has a half-life of 0.1−1.75 h and is a prodrug of valdecoxib. [d] In dog.

of the inhibitor inside the active site, so that an ideal combination of properties is obtained.

CONCLUSIONS

This paper represents the first attempt to observe the movement of a ligand from the active site of a protein to its exterior using MD techniques and to identify local minima along the ligand path. (1) This study involves MD runs amounting to a total time of ∼5 ns at 1 fs intervals with ∼100 residues, 160 water molecules, and the SC-558 ligand. Also, it involves the analysis of 154 minimized conformations. (2) The method of incremental movement of the ligand, from the active site to the exit through the gate and cavity, which we adopted seems to be realistic because the ligand can explore different possible potential minima in each MD run; the lowest energy path is then effectively mapped. (3) The movement of the ligand is not haphazard but, rather, obeys the grammar of hydrogen bonding. The anticooperative arrangements show that the ligand movement takes place with the breaking and making of hydrogen bonds in a relay fashion. (4) The ligand path may be divided into three stages. In each, the ligand has a characteristic conformation and orientation. (5) The existence of a gate and a distinct cavity have been emphatically proven by this ligand coordinate analysis. The movements of different residues that characterize the gate have also been understood. (6) The importance of water is explicit. The ligand forms many strong hydrogen bonds with water. During the later stages, water aids in forming a capsulelike environment around the ligand that possibly favors ligand exit. (7) The interactions/contacts formed by the CF_3 group are enigmatic and pose a question for future work. (8) The protein breathes and loosens as soon as the ligand leaves the active site, and this could have to do with the enthalpy−entropy balance. (9) This study has implications on the residence time of the ligand in the active site that, in turn, could be related to the adverse cardiovascular effects observed in selective COX-2 inhibitors.

While MD is clearly the preferred approach for studies of this kind, questions of reproducibility, reversibility, and generality are pertinent because these questions have a direct bearing on the methodology itself. However, we conclude by stating that this exercise is a statistical treatment of events and that we have elucidated a ligand pathway that is generally correct, even if some of the finer details may change with slightly different protocols in the methodology. In particular, we assert that what is important is that the geometry in the 8.2 Å position is an unusual one, in that the ligand is strained. Could one assume that this could represent a putative supramolecular transition state? How exactly the ligand is distorted, what the exact energy barrier is, and how the interactions look precisely at this particular position may be revised in future. However, what is significant is that the pathway of the ligand through the enzyme has a "choke point" at this 8.2 Å distance. This is amply borne out by the fact that the entire system behaves normally at all of the other positions. This idea of a "choke point" is also chemically reasonable. This paper may be considered, therefore, as an early attempt to quantify the events involved with ligand movement in an enzyme.

Supporting Information Available: Snapshots of protein−ligand interactions in stereoview are given Figures S1−S11; ligand−residue and ligand−water interaction metrics are given in Table 1. An animated sequence of 120 frames (10 minima in each of the 12 runs) as a movie is also provided. This material is available free of charge via the Internet at http://pubs.acs.org.

ACKNOWLEDGMENT

K.V.V.M.S.R. thanks the CSIR for an SRF and Dr. R. Mukherjee, Dabur Research Foundation, for her support. G.R.D. thanks the DST and the UGC for support under the UPE (CMSD). J.A.R.P.S. and G.R. thank Mr. G. V. Sanjay Reddy, GVK Biosciences, for his support and encouragement.

REFERENCES AND NOTES

(1) Simmons, D. L.; Botting, R. M.; Hla, T. Cyclooxygenase Isozymes: The Biology of Prostaglandin Synthesis and Inhibition. *Pharm. Rev.* **2004**, *56*, 387−437.

(2) Vane, J. R.; Botting, R. Mechanism of Action of Antiinflammatory Drugs. *Scand. J. Rheumatol. Suppl.* **1996**, *102*, 9−21.
(3) FitzGerald, G. A. Coxibs and Cardiovascular Disease. *N. Engl. J. Med.* **2004**, *351*, 1709−1711.
(4) Solomon, D. H.; Schneeweiss, S.; Glynn, R. J.; Kiyota, Y.; Levin, R.; Mogun, H.; Avron, J. Relationship between Selective Cyclooxygenase-2 Inhibitors and Acute Myocardial Infarction in Older Adults. *Circulation* **2004**, *109*, 2068−2073.
(5) Davies, N. M.; Jamali, F. COX-2 Selective Inhibitors Cardiac Toxicity: Getting to the Heart of the Matter. *J. Pharm. Pharm. Sci*. **2004**, *7*, 332−336.
(6) Finckh, A.; Aronson, M. D. Cardiovascular Risks of Cyclooxygenase-2 Inhibitors: Where We Stand Now. *Ann. Intern. Med.* **2005**, *142*, 212−214.
(7) Dogne, J. M.; Supuran, C. T.; Pratico, D. Adverse Cardiovascular Effects of the Coxibs. *J. Med. Chem.* **2005**, *48*, 2251−2257.
(8) FitzGerald, G. A. COX-2 and Beyond: Approaches to Prostaglandin Inhibition in Human Disease. *Nat. Rev. Drug Discovery* **2003**, *2*, 879−902.
(9) Black, W. C. Selective Cyclooxygenase-2 Inhibitors. *Annu. Rep. Med. Chem.* **2004**, *39*, 125−138.
(10) Price, M. L. P.; Jorgensen W. L. Analysis of Binding Affinities for Celecoxib Analogues with Cox-1 and Cox-2 from Combined Docking and Monte Carlo Simulations and Insight into the Cox-2/Cox-1 Selectivity. *J. Am. Chem. Soc.* **2000**, *122*, 9455−9466.
(11) Solvia, R.; Almansa, C.; Kalko, S. G. Luque, F. J.; Orozco, M. Theoretical Studies on the Inhibition Mechanism of Cyclooxygenase-2. Is There a Unique Recognition Site? *J. Med. Chem.* **2003**, *46*, 1372−1382.
(12) Llorens, O.; Perez, J. J.; Palomer, A.; Mauleon, D. Structural Basis of the Dynamic Mechanism of Ligand Binding to Cyclooxygenase. *Bioorg. Med. Chem. Lett*. **1999**, *9*, 2779−2784.
(13) Desiraju, G. R.; Gopalakrishnan, B.; Jetti, R. K. R.; Nagaraju, A.; Raveendra, D.; Sarma, J. A. R. P.; Sobhia, M. E.; Thilagavathi, R. Computer-Aided Design of Selective COX-2 Inhibitors: Comparative Molecular Field Analysis, Comparative Molecular Similarity Indices Analysis, and Docking Studies of Some 1, 2-Diarylimidazole Derivatives. *J. Med. Chem.* **2002**, *45*, 4847−4857.
(14) Llorens, O.; Perez, J. J.; Palomer, A.; Mauleon, D. Differential Binding Mode of Diverse Cyclooxygenase Inhibitors. *J. Mol. Graphics Modell*. **2002**, *20*, 359−371.
(15) Lanzo, C. A.; Sutin, J.; Rowlinson, S.; Talley, J.; Marnett, L. J. Fluorescence Quenching Analysis of the Association and Dissociation of a Diarylheterocycle to Cyclooxygenase-1 and Cyclooxygenase-2: Dynamic Basis of Cyclooxygenase-2 Selectivity. *Biochemistry* **2000**, *39*, 6228−6234.
(16) Kurumbail, R. G.; Stevens, A. M.; Gierse, J. M.; McDonald, J. J.; Stegeman, R. A.; Pak, J. Y.; Gildehaus, D.; Miyashiro, J. M.; Penning, T. D.; Seibert, K.; Isakson, P. C.; Stallings, W. C. Structural Basis for Selective Inhibition of Cyclooxygenase-2 by Antiinflammatory Agents. *Nature* **1996**, *384*, 644−648.
(17) Xu, Y.; Shen, J.; Luo, X.; Silman, I.; Sussman, J. L.; Chen, K.; Jiang, H. How Does Huperzine A Enter and Leave the Binding Gorge of Acetylcholinesterase? Steered Molecular Dynamics Simulation. *J. Am. Chem. Soc.* **2003**, *125*, 11340−11349.
(18) Camacho, C. J.; Vajda, S. Protein Docking along Smooth Association Pathways. *Proc. Natl. Acad. Sci. U.S.A.* **2001**, *98*, 10636−10641.
(19) Deka, R. C.; Vetrivel, R. Adsorption Sites and Diffusion Mechanism of Alkylbenzenes in Large Pore Zeolite Catalysts as Predicted by Molecular Modeling Techniques. *J. Catal.* **1998**, *174*, 88−97.
(20) Steiner, T.; Koellner, G. Coexistence of Both Histidine Tautomers in the Solid State and Stabilization of the Unfavourable Nδ−H Form by Intramolecular Hydrogen Bonding: Crystalline L-His-Gly Hemihydrate. *Chem. Commun.* **1997**, 1207−1208.
(21) *MOE 2002.03*; Chemical Computing Group Inc.: Montreal, Canada.
(22) *Cerius*^{2}; Accelrys Ltd.: Cambridge, U. K.
(23) *Insight II*; Accelrys Ltd.: Cambridge, U. K.
(24) At each new position, *r*, *w*, *L*, and *U* are set as 1, 9, −0.1, and 0.1, respectively. This upper and lower interval is a "flat-bottomed" restraint in that the force is zero inside the interval and large outside. At each point, A_d was considered as the new *r*.
(25) Simmons, D. L.; Botting, R. M.; Hla, T. Cyclooxygenase Isozymes: The Biology of Prostaglandin Synthesis and Inhibition. *Pharmacol. Rev.* **2004**, *56*, 387−437.
(26) Rowlinson, S. W.; Kiefer, J. R.; Prusakiewicz, J. J.; Pawlitz, J. L.; Kozak, K. R.; Kalgutkar, A. S.; Stallings, W. C.; Kurumbail, R. G.; Marnett, L. J. A Novel Mechanism of Cyclooxygenase-2 Inhibition Involving Interactions with Ser-530 and Tyr-385. *J. Biol. Chem.* **2003**, *278*, 45763−457639.
(27) Selinsky, B. S.; Gupta, K.; Sharkey, C. P.; Loll, P. J. Structural Analysis of NSAID Binding by Prostaglandin H_2 Synthase: Time-Dependent and Time-Independent Inhibitors Elicit Identical Enzyme Conformations. *Biochemistry* **2001**, *40*, 5172−5180.
(28) Pouplana, R.; Lozano, J. J.; Perez, C.; Ruiz, J. Structure-Based QSAR Study on Differential Inhibition of Human Prostaglandin Endoperoxide H Synthase-2 (COX-2) by Nonsteroidal Antiinflammatory Drugs. *J. Comput.-Aided Mol. Des.* **2002**, *16*, 683−701.
(29) Jeffrey, G. A. In *An Introduction to Hydrogen Bonding*; Oxford University Press: New York, 1997.
(30) Dunitz, J. D.; Taylor, R. Organic Fluorine Hardly Ever Accepts Hydrogen Bonds. *Chem.*−*Eur. J*. **1997**, *3*, 89−98.
(31) Thalladi, V. R.; Weiss, H. C.; Blaser, D.; Boese, R.; Nangia, A.; Desiraju, G. R. C−H···F Interactions in the Crystal Structures of Some Fluorobenzenes. *J. Am. Chem. Soc*. **1998**, *120*, 8702−8710.
(32) Hof, F.; Diederich, F. Medicinal Chemistry in Academia: Molecular Recognition with Biological Receptors. *Chem. Commun.* **2004**, 477−480.
(33) Kui, S. C. F.; Zhu, N.; Chan, M. C. W. Observation of Intramolecular C−H···F−C Contacts in Nonmetallocene Polyolefin Catalysts: Model for Weak Attractive Interactions between Polymer Chain and Noninnocent Ligand. *Angew. Chem., Int. Ed.* **2003**, *42*, 1628−1632.
(34) Sarma, J. A. R. P.; Dunitz, J. D. Structures of Three Crystalline Phases of *p*-(Trimethylammonio)benzenesulfonate and Their Interconversions. *Acta Crystallogr., Sect. B* **1990**, *46*, 784−794.
(35) Jeffrey, G. A. In *Comprehensive Supramolecular Chemistry*; MacNicol, D. D., Toda, F., Bishop, R., Ed.; Pergamon: Oxford, U. K., 1996; Vol. 6, pp 757−788.
(36) Dunitz, J. D. Win Some, Lose Some: Enthalpy−Entropy Compensation in Weak Intermolecular Interactions. *Chem. Biol.* **1995**, *2*, 709−712.
(37) Williams, D. H.; Stephens, E.; Zhou, M. How Can Enzymes Be So Efficient? *Chem. Commun.* **2003**, 1973−1976.
(38) Drug Database and Clinical Candidate Database; GVK Biosciences Pvt. Ltd.: Hyderabad, India, 2005.
(39) Benet, L. Z.; Perotti, B. Y. T. In *Burger's Medicinal Chemistry and Drug Discovery*; Wolff, M. E., Ed.; Wiley: New York, 1995; Vol. 1, Chapter 5, pp 121−122.
(40) Krötz, F.; Schiele, T. M.; Klauss, V.; Sohn, H.-Y. Selective COX-2 Inhibitors and Risk of Myocardial Infarction. *J. Vasc. Res.* **2005**, *42*, 312−324.

CI050142I